Two-photon fluorescence imaging of DNA in living plant turbid tissue with carbazole dicationic salt†

Yuanhong Zhang,[a] Junjie Wang,[a] Pengfei Jia,[b] Xiaoqiang Yu,*[a] Heng Liu,*[b] Xin Liu,[a] Ning Zhao[a] and Baibiao Huang*[a]

Received 22nd April 2010, Accepted 30th June 2010
DOI: 10.1039/c0ob00030b

Three carbazole dicationic salts, namely 3,6-bis(1-methyl-4-vinylpyridinium) carbazole diiodide (BMVC), 9-ethyl-3,6-bis(1-methyl-4-vinylpyridinium) carbazole diiodide (9E-BMVC) and 9-ethyl-3,6-bis(1-hydroxyethyl-4-vinylpyridinium)carbazole diiodide (9E-BHVC), were synthesized successfully. Their photophysical properties were evaluated by absorption, one- and two-photon fluorescence spectra, and their higher fluorescence intensity and larger two-photon excited fluorescence action cross-sections ($\Phi \times \delta$) in the presence of DNA than those in the absence of DNA give them good DNA two-photon light-switch properties. Furthermore, their ability to image nuclei in living plant cells and turbid tissues by using two-photon excited fluorescence was carefully studied, and the experimental results indicate that these dicationic salts can exclusively label nuclei in intact living plant cells and tissues. In particular, 9E-BHVC exhibits optimized DNA labeling performance. Very importantly, compared to DAPI, 9E-BHVC can be used to carry out deeper observation using the same incident power, or can be used to obtain usable fluorescent images by using a lower incident power.

Introduction

Two-photon fluorescence microscopy (TPM)[1] has raised expectations for the observation of living phenomena in entire organs and tissues.[2] A recent comparison study has convincingly demonstrated that TPM is superior to confocal microscopy in the imaging of thick and highly scattering specimens.[3] For example, TPM has been used to visualize both autofluorescence and exogenous fluorophores in human skin.[4] Although confocal imaging enables the imaging of dental biofilm down to a depth of 40 μm, two-photon excitation images could be recorded at a depth even greater than 100 μm.[5] Recently, Feijó and Cox investigated the meiotic events in intact living anthers of *Agapanthus umbelatus* using DAPI as the DNA fluorescent probe.[6] The images obtained with TPM provided a deeper understanding and more details of the meiotic process *in vivo*.[7] However, the authors also recognized that they could not optimize the visualization to a degree that was capable of observing the vital signs of meiotic events, especially the meiotic progression in the sporogenic tissue of the plants. One possible reason is that the high incident power needed to penetrate such thick specimens could disturb the normal meiotic process. As a result, conventional fluorescent probes are not suitable for the imaging of thick samples due to their small two-photon excited fluorescence action cross-sections ($\Phi \times \delta$).[8] Theoretically, as OPE (one photon excitation) and TPE (two-photon excitation) obey different selection rules,[9] one cannot expect conventional OPE probes to necessarily have optimized properties for TPE. Therefore, to image deep inside tissue, the design and synthesis of new fluorescent probes with large $\Phi \times \delta$ have attracted considerable interest.[10]

Nucleic acids are important life substances relevant to analytical and diagnostic applications,[11] and a few fluorescent probes of DNA with optimized two-photon fluorescent properties have been reported.[12] Allain *et al.*[13] described some two-photon active DNA probes with far-red emission of 660–680 nm, and Φ of 0.066 and δ of 200 GM (measurements in the presence of herring testes DNA). They double-stained the paraformaldehyde-fixed CHO K1 cells with their own two-photon fluorescent probes and commercially available DAPI. The photos from epifluorescence microscopy indicated that the obtained new probes possess the expected special ability of nuclei labeling. More recently, a two-photon fluorescent probe, *i.e.* 3,6-bis(1-methyl-4-vinylpyridinium) carbazole diiodide (BMVC) aimed at monitoring telomeres and their G-quadruplex structure *in vitro* has been introduced by Chang *et al.*[14] Based on BMVC, they have obtained a mitochondrial probe, *i.e.* 9P-BMVC, and its imaging ability in cells has been primarily proved in the wide-field fluorescence microscopy.[15] Chang *et al.* suggested that substitutuents at the 9-position of BMVC with different electronic properties could affect its photophysical properties and

[a]*State Key Laboratory of Crystal Materials, Shandong University, Jinan, 250100, China. E-mail: yuxq@sdu.edu.cn, bbhuang@sdu.edu.cn*
[b]*MOE Key Laboratory of Arid and Grassland Ecology, Institute of Cell Biology, Life Science School, Lanzhou University, Lanzhou, 730000, China. E-mail: hengliu@lzu.edu.cn*

† Electronic supplementary information (ESI) available: Experimental details and characterization of the three compounds, preparation and staining of living plant cells and tissue, measurement equipment and methods, TPM experiment, measurement of TPA cross sections, measurement of binding parameters, photophysical properties, electronic absorption and one-photon fluorescence spectra in various solvents, electronic absorption of the three compounds' titration with DNA, analysis of binding parameters, TPM pictures of protoplasts incubated with 9E-BMVC/BMVC and DAPI, TPM pictures of root tip incubated with 9E-BHVC, optical sections of intact *Arabidopsisi* hypocotyls double-stained by 9E-BHVC and DAPI at different depths, optical sections of intact *Arabidopsis* root double-stained by 9E-BHVC and DAPI at different depths, microscopic photos of intact *Arabidopsis* root double-stained by 9E-BHVC and DAPI at different power. See DOI: 10.1039/c0ob00030b

Table 1 The photophysical properties of 9E-BHVC, 9E-BMVC, BMVC and DAPI

Sample	Solvent	λ^1_{max}/nm	λ^2_{max}/nm	λ^3_{max}/nm	Abs/a.u	ε/M^{-1} cm^{-1}	Φ [%][a]	δ/GM[b]	$\Phi\times\delta$/GM[c]
9E-BHVC	Acetone	455	586	602	0.18	7.22×10^4	4.18	220	9.2
	Acetonitrile	455	592	603	0.19	7.71×10^4	2.73	1280	34.9
	Ethanol	463	578	598	0.19	7.63×10^4	8.10	1170	94.8
	DMF	455	593	599	0.18	7.11×10^4	2.42	600	14.5
	Water	451	566	586	0.15	6.13×10^4	0.11	820	0.9
	Buffer	451	566	642	0.18	4.42×10^4	0.11	2200[e]	2.4[e]
	DNA[d]	474	540	573	0.23	5.63×10^4	38.9	230[e]	89.5[e]
9E-BMVC	Acetone	452	587	589	0.19	7.55×10^4	2.87	380	10.9
	Acetonitrile	450	596	604	0.18	7.35×10^4	1.97	1270	25.0
	Ethanol	461	583	596	0.18	7.20×10^4	6.24	670	41.8
	DMF	451	595	597	0.17	6.82×10^4	1.59	360	5.7
	Water	444	586	596	0.15	6.02×10^4	0.14	1310	1.8
	Buffer	444	565	609	0.15	3.06×10^4	0.23	1500[e]	3.5[e]
	DNA[d]	464	541	575	0.22	4.35×10^4	30.8	311[e]	95.8[e]
BMVC	Acetone	443	574	591	0.15	6.14×10^4	1.60	210	3.4
	Acetonitrile	438	579	601	0.19	7.50×10^4	1.14	670	7.6
	Ethanol	458	569	592	0.20	7.94×10^4	3.97	550	21.8
	DMF	445	583	602	0.18	7.11×10^4	0.79	290	2.3
	Water	434	565	584	0.16	6.22×10^4	0.09	660	0.6
	Buffer	434	554	597	0.19	3.77×10^4	0.07	1600	1.1
	DNA[d]	456	534	556	0.25	5.05×10^4	23.6	190	44.8
DAPI	Acetone	353	456	476	0.13	1.25×10^4	2.81	2.25	0.063
	Acetonitrile	348	461	476	0.15	1.53×10^4	9.24	0.77	0.071
	Ethanol	351	452	457	0.31	3.07×10^4	78.6	2.48	1.95
	DMF	351	460	467	0.29	2.93×10^4	53.2	8.62	4.59
	Water	343	459	489	0.28	2.78×10^4	2.79	0.66	0.018 (ref. 19)
	Buffer	344	454	489	0.28	2.80×10^4	2.83	0.82	0.023
	DNA[d]	359	455	473	0.20	2.04×10^4	60.5	3.60	2.18

λ^1_{max}, λ^2_{max} and λ^3_{max} are linear absorption, single- and two-photon fluorescent maximum peaks, respectively. Abs is absorbance. ε is molar absorptivity. Φ is single-photon fluorescence quantum yield determined using fluorescein ($\Phi = 0.95$) as the standard. δ and $\Phi\times\delta$ are two-photon absorption cross-sections and two-photon excited fluorescence action cross-sections determined using fluorescein (δ = 36 GM)[19] at 800 nm. Those for DAPI are determined at 800 nm using coumarin 307 in methanol (Φ = 0.56, δ = 27.7 GM[8a]) as the standard. 1 GM = 10^{-50} cm^4 s photon^{-1}.[a] Error limit: 10%. [b] Error limit: 20%. [c] Error limit: 32%. [d] In tris-HCl buffer in the presence of calf-thymus DNA, the values of *phosphate of DNA/dye*: 70 for 9E-BHVC, 30 for 9E-BMVC and 40 for BMVC, 40 for DAPI. Concentration of samples for δ and $\Phi\times\delta$: 100 μM. [e] Concentration: 50 μM

cellular responses. More recently, we found that 9-ethyl-3,6-bis(1-methyl-4-vinylpyridinium) carbazole diiodide (9E-BMVC) with two-photon DNA "light-switch" properties can label nuclei in fixed cancer cells.[16]

It is very important to image living thick and turbid plant tissue using a fluorophore with a large $\Phi\times\delta$, but, so far, no relevant research is reported. In this paper, we investigated the imaging ability of three carbazole dicationic salts in detail in living turbid plant tissue; these dicationic salts include BMVC, 9E-BMVC and 9-ethyl-3,6-bis(1-hydroxyethyl-4-vinylpyridinium)carbazole diiodide (9E-BHVC). The molecular structures of 9E-BHVC, 9E-BMVC, BMVC and DAPI are shown in Chart 1.

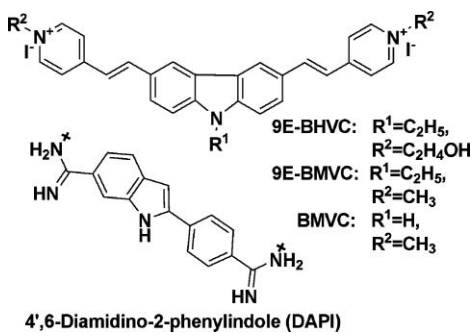

Chart 1 Chemical structures of 9E-BHVC, 9E-BMVC, BMVC and DAPI.

The optical properties of the three derivatives in various solvents were evaluated by absorption, and one- and two-photon fluorescent spectra. The experimental results show that they have large $\Phi\times\delta$ in the presence of DNA (45–96 GM) and high affinity for DNA (10^6–10^7 M^{-1}), which rank them as the best two-photon fluorescent DNA probes. Interestingly, these compounds are only weakly fluorescent in water, whereas their two-photon fluorescence emissions are strongly restored (36–49-fold enhancement) upon binding to DNA. Finally, the nuclear imaging properties of these compounds in living plant cell and tissue reveal that they can exclusively label nuclei. Experimental results show that carbazole dicationic salts should be promising for fluorophore imaging of turbid and thick biological specimens. Among the three compounds in this paper, 9E-BHVC is attractive for application as a two-photon fluorescent DNA stain in living plant tissue.

Results and discussions

Photophysical properties in various solvents

The synthetic route to 9E-BHVC and 9E-BMVC has been given in Scheme S1† and the relevant photophysical properties of three compounds are summarized in Table 1. Their maximum linear absorption wavelengths in various polarity solvents are in the range of 434–474 nm (Fig. S1†), thus the two-photon absorptions

of these derivatives can be excited by Ti:sapphire laser sources tuneable in the range 740–900 nm. From Table 1, one can also find that their fluorescent quantum yields (Φ) are high in organic solvents and very low in aqueous solutions. Additionally, their Φ values in glycerol with high viscosity, about 13.1% (9E-BHVC), 11.6% (9E-BMVC) and 10.0% (BMVC), are obviously higher than those in other organic solvents. This may be attributed to the high viscosity of the medium, which can hinder the torsional motion of the vinyl groups in these derivatives and thus increase the Φ values.

All these characteristics mean that these compounds may have DNA "light-switch" effects,[17] since the dyes will be in an organic environment and their torsional motion will also be restricted when incorporated into the hydrophobic grooves of DNA.[13a] According to Table 1, similar to one-photon fluorescence properties, the fluorescence by two-photon excitation exhibits evident solvatochromism, and higher two-photon fluorescence intensity of the three dyes in organic solvents than those in water are also found (Fig. 1). This indicates that they may have two-photon DNA "light-switch" effects.

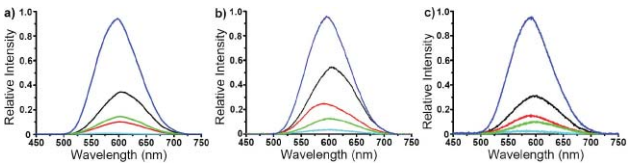

Fig. 1 Two-photon fluorescence spectra of 9E-BHVC (a), 9E-BMVC (b), and BMVC (c) in various solvents. [Compound] = 100 μM. Blue: EtOH, black: MeCN, green: DMF, red: acetone, and cyan: water. Excitation wavelength, 800 nm. Error limit: 8%.

For a compound used as a two-photon fluorescence probe, the efficiency with which a fluorophore absorbs and emits photons is represented by the two-photon absorption (TPA) cross-sections, (δ) for absorption and the Φ for fluorescence. Fluorescence intensity per fluorophore is proportional to the product of δ and Φ. The three fluorophores possess bigger $\Phi \times \delta$ in comparison with commercial DNA dyes, such as DAPI in water (0.16 GM, excitation wavelength: 700 nm)[8a,8b,10a] and other solvents (Table 1). Furthermore, the data in Table 1 also show that $\Phi \times \delta$ of 9E-BHVC and 9E-BMVC are greater than that of BMVC in various environments due to the ethyl group with donor properties in the place of the H atom of the carbazole motif.[18] In the presence of calf thymus DNA, the $\Phi \times \delta$ values exhibited by 9E-BHVC, 9E-BMVC and BMVC are 90, 96 and 45 GM (Table 1), which are 38-, 29- and 41-fold enhancements of those in tris-HCl buffer. This demonstrates that these derivatives can be used as two-photon fluorescence "light switch" for DNA. Moreover, the excited spectra of δ and $\Phi \times \delta$ of the three compounds and DAPI in various solvents have been plotted in Fig. 2. Both δ and $\Phi \times \delta$ from the three carbazole dicationic salts are always higher than those of DAPI at various excitation wavelengths and in various environments. When the excitation wavelengths are between 800–820 nm, the compounds exhibit higher δ and $\Phi \times \delta$. Amongst the compounds, 9E-BHVC shows the best properties.

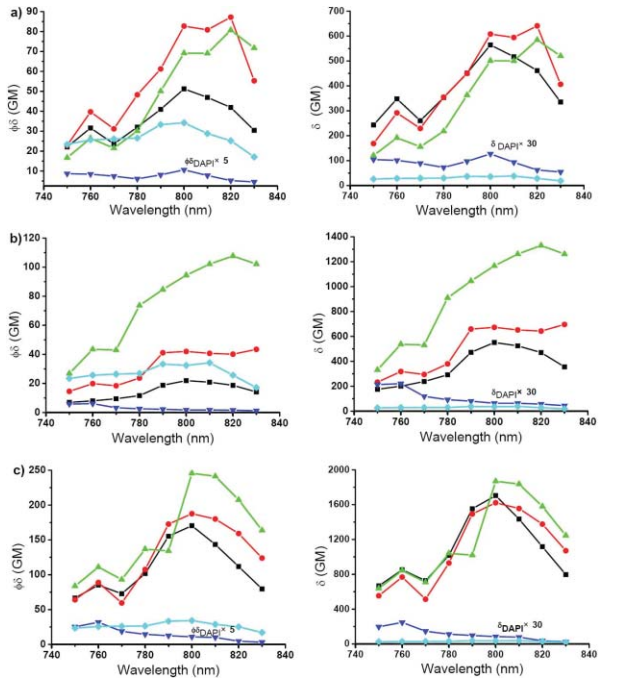

Fig. 2 Excitation spectra of two-photon excited fluorescence action cross-sections (left, error limit: 32%) and two-photon absorption cross–sections (right, error limit: 20%) for 9E-BHVC (green triangle), 9E-BMVC (red circle), BMVC (black square) and DAPI (blue triangle) in various solvents. In the measurements, fluorescein (pH = 11, cyan diamond) in aqueous NaOH is used as standard.[8a] a) tris-HCl buffer (10 mM, pH 7.2, KCl 100 mM) in the presence of calf-thymus DNA (*phosphate of DNA/dye* = 10); b) EtOH and c) glycerol. [Compound] = 10 μM in the presence of DNA, 100 μM in ethanol and 50 μM in glycerol.

DNA titration

To check the possibility of using the three compounds as two-photon fluorescent DNA probes, fluorescence titration experiments have been carried out, and calf thymus DNA was used as the model. The results obtained are shown in Fig. 3, and the data are listed in Table 1. Delightfully, in both one-photon and two-photon fluorescence titration, the fluorescence intensity evidently increases with the addition of DNA. We think that two factors can explain the mechanism of the light-up effect of the dyes binding to DNA. Firstly, dyes that are in a twist intramolecular charge transfer (TICT) state whose non-radiative process quenches the fluorescence will be non-emissive; inversely, dyes for which the formation of a TICT state is restricted become brightly luminescent.[20] For these dyes, the intramolecular charge transfer (ICT) state could occur between the electron donor of the carbazole moiety and the electron acceptor of the pyridinium cation.[21] Once in water, the larger dipole moment in the excited state than that in the ground state interacts strongly with the polar solvent, which could lead to charge separation resulting in formation of a TICT state. However, the formation of a TICT state is restricted when the dye is protected from water in the grooves of DNA, and the fluorescence of the dyes will be restored. On the other hand, the rapid non-radiative decay that results from the torsional motion of the fluorophore will be responsible for the low quantum yield of the TICT states in numerous dyes.[22] When binding to DNA, the torsional motion of vinyl groups can be

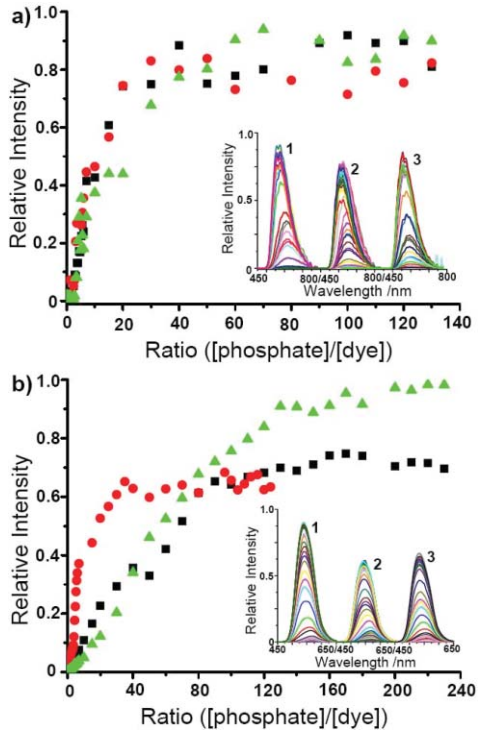

Fig. 3 Two- (a) and one-photon (b) fluorescence exaltation of 9E-BHVC (green triangle)/9E-BMVC (red circle)/BMVC (black square) with the addition of calf-thymus DNA. Insert: 1, 2 and 3 are the corresponding fluorescent spectra of 9E-BHVC, 9E-BMVC and BMVC. a, Change curves of two-photon excitation. [9E-BHVC] = [9E-BMVC] = 50 μM, [BMVC] = 100 μM, [phosphate in DNA] = 0–6.5 mM for 9E-BHVC/9E-BMVC, 0–13 mM for BMVC. Excitation wavelength, 800 nm. Buffer, 10 mM Tris-HCl, 100 mM KCl, pH = 7.2. Each point shown has an error of 8%. b, Change curves of single-photon excitation. Dye concentration, 2.5 μM, [phosphate in DNA] = 0–600 μM for 9E-BHVC/BMVC, 0–310 μM for 9E-BMVC. Excitation wavelength, 425 nm. Buffer, idem.

restricted by the steric effect deriving from the static interactions between the cationic N-pyridinium and the anionic phosphate of DNA, and the interaction of grooves combining in the double helices, thus the fluorescence can increase.

Moreover, the strong interaction between the compounds and DNA is further confirmed by absorption titration (Fig. S2†).[23] With the addition of DNA, the three molecules show significant bathochromic shifts[24] (20–23 nm) and large absorbance changes in opposite directions.[25] We think that the fall of the excited energy level due to the interaction to DNA[26] can explain this red-shift phenomenon. In addition, the intrinsic binding constants (k) to DNA have been obtained by analyzing the one-photon fluorescence titration data with the Scatchard equation[27] (Fig. S3 in the ESI†). The k values of 9E-BHVC, 9E-BMVC and BMVC are 1.02×10^7, 6.4×10^6 and 6.7×10^6 M^{-1}, which are comparable to 10^6 M^{-1} of DAPI to DNA.[28] The best DNA-binding properties of 9E-BHVC can be attributed to the formation of H-bonds between the H atoms of hydroxylethyl groups and the base pairs in DNA.[29]

The two-photon fluorescence intensities of 9E-BHVC, 9E-BMVC and BMVC at saturation are 54-, 36- and 49-fold enhancements of those in tris-HCl buffer, respectively. 485- (9*E*-BHVC), 83- (9*E*-BMVC) and 374-fold (BMVC) enhancements are found for one-photon excitation. Therefore, one can reasonably expect that, after permeating into living cells and/or tissues, the three compounds bound to DNA will emit more intensive luminescence than those staying in the cytoplasm. That is to say, the three compounds should be good two-photon fluorescent probes for DNA, if they can specifically label DNA in living cells and tissues. Considering that 800 nm is an optimal excitation wavelength provided by a commercial mode locked Ti:sapphire laser source used in TPM, this wavelength will be chosen as the excitation wavelength to image DNA in living cells and tissues.

Imaging DNA in living plant cells and tissues

To investigate the specificity of these dicationic salts in labeling DNA in imaging nuclei in living plant cells and tissues utilizing TPM, selecting *Arabidopsis thaliana*,[30] a model plant, as the specimen is rational. Firstly, the cell detection has been carried out in protoplasts. The double-staining photo of 9E-BHVC is given in Fig. 4, that of 9E-BMVC and BMVC are in Fig. S4.† The results show that they can stain the DNA in protoplasts which have been isolated from callus of *Arabidopsis thaliana* leaves (see the ESI†), and the position and region stained are consistent with those of DAPI.

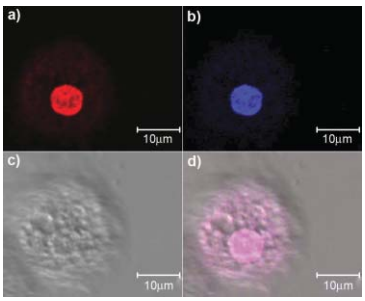

Fig. 4 TPM pictures of protoplasts incubated with 9E-BHVC and DAPI for 0.5 h. a, 9E-BHVC (1 μM, 2% incident power). b, DAPI (1 μM, 5% incident power). c, Phase-contrast picture. d, Merged picture. Excitation wavelength, 800 nm. Detection wavelength, 435–485 nm (DAPI), 535–590 nm (9E-BHVC). The percentages of incident power mentioned above are the power output of AOM in LSM 510META of Zeiss. See the ESI for details.†

No distinct difference between the three compounds is found when staining protoplasts of *Arabidopsis thaliana*. However, when staining living tissue of *Arabidopsis thaliana*, the abilities of 9E-BHVC and 9E-BMVC are superior to BMVC, and 9E-BHVC should be best. From Fig. 5 and Fig. S5,† one can see that the 9E-BHVC labels almost all nuclei in the root tip, comparatively the amount of nuclei stained by BMVC is small.

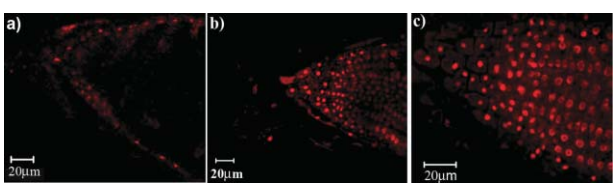

Fig. 5 Fluorescence images of the root tip incubated with BMVC (a), 9E-BMVC (b) and 9E-BHVC (c), for 1 h at 5 μM. Incident power: 1%. Excitation wavelength, 800 nm. Detection wavelength, 535–590 nm.

At the same time, 9E-BHVC can successfully stain many parts of the living tissue of *Arabidopsis thaliana*, such as hypocotyls and roots shown in Fig. 6 (autofluorescence from cell walls of the hypocotyl is also visible[6]). In Video S1,† 24 optical sections of hypocotyls double-stained by 9E-BHVC and DAPI were constructed. These photos have expressly demonstrated that 9E-BHVC can bind selectively to DNA, and the positions and amounts of the nuclei labelled by 9E-BHVC are exactly the same as those of DAPI.

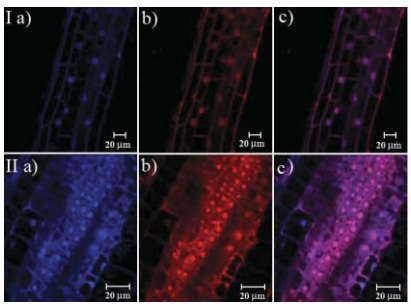

Fig. 6 TPM pictures of hypocotyls at 13 μm (I) and roots at 18 μm (II) incubated with 9E-BHVC and DAPI for 1 h. Ia, DAPI (2 μM, 5% incident power). Ib, 9E-BHVC (1 μM, 5% incident power). IIa, DAPI (3 μM, 4% incident power). IIb, 9E-BHVC (3 μM, 2% incident power). Ic and IIc, merged pictures. Detection wavelength, 435–485 nm (DAPI), 535–590 nm (9E-BHVC). Excitation wavelength, 800 nm.

Compared to confocal microscopy, the lower photodamage and deeper penetration should be the most noticeable advantages of TPM, which result from both the red-shift incident laser wavelength and the smaller excited volume in specimen. However, conventional fluorescent probes with small $\Phi \times \delta$ have brought some new problems; for example, the incident laser power has to be increased in order to acquire an improved image from two-photon fluorescence. Hence, when one uses a conventional single-photon fluorescent probe with smaller $\Phi \times \delta$ to image living tissue utilizing TPM, only a small amount of the incident laser power absorbed by probes can be used to emit fluorescence, a lot of energy is transformed into thermal energy and results in heat damage to the specimen. On the other hand, the imaging depth of the detected tissue is affected by not only the penetration distance of the incident beam into specimen, but also by the fluorescence intensity and emission wavelength of the probes, especially in turbid specimens. Thus, in order to image deeper sections of turbid tissue, the advantageous two-photon fluorescent properties and red-shifted fluorescence emission of the probes should be two crucial factors.

To examine the imaging ability difference between 9E-BHVC and DAPI in imaging highly scattering specimens, a series of double-staining experiments have been carried out in the turbid root of *Arabidopsis thaliana*. Fig. 7A gives a series of double-staining microscopic photos of DAPI and 9E-BHVC under the same imaging conditions and at different depths. These results show again the exact consistency of labeling positions and amounts of 9E-BHVC and DAPI in the living plant turbid tissue. According to Fig. 7AI, at 13 μm depth, the fluorescence of 9E-BHVC is a little excessive while the fluorescence of DAPI is just visible. Furthermore, at 23 μm, the image of 9E-BHVC is visible and the fluorescence of DAPI is invisible (Fig. 7AII). At 18 μm

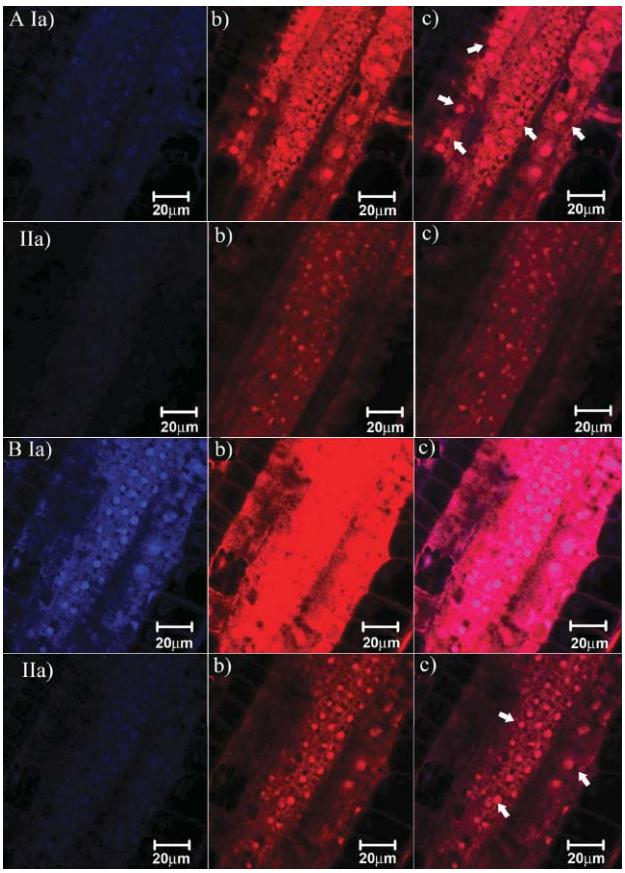

Fig. 7 TPM pictures of Arabidopsis roots incubated for 1 h with 3 μM of 9E-BHVC/DAPI at different depths with 2% incident power (A) and with different incident power at 18 μm (B). AI, $Z = 13$ μm. AII, $Z = 23$ μm. BI, Incident power: 4%. BII, Incident power: 2%. a, DAPI. b, 9E-BHVC. c, Merged picture. Excitation wavelength: 800 nm. Detection wavelength, 435–485 nm (DAPI), 535–590 nm (9E-BHVC).

depth, in order to obtain a usable image from DAPI, the incident power has to increase to 4%, but at this power the fluorescence of 9E-BHVC is saturated (Fig. 7BI). To 9E-BHVC, the usual incident power of usable image is 2%, and at this energy the florescence of DAPI is invisible (Fig. 7BII). In 4% and 2% of incident power, the fluorescence photos of root at 18 μm from DAPI and 9E-BHVC have been obtained, respectively (Fig. 6II).

To investigate and compare the two-photon fluorescent imaging depths of 9E-BHVC and DAPI in *Arabidopsis* root, 41 optical sections of root of different depths double-stained by 9E-BHVC and DAPI have been obtained. The photos in Fig. 7A were used to construct Video S2.† In the 41 sections we randomly selected five nuclei indicated by arrows in Fig. 7AIc. The fluorescence intensity of 9E-BHVC and DAPI on the five nuclei in the 41 sections was determined. The relationship between the average values of five intensity measurements of 9E-BHVC or DAPI at the same section and imaging depths were plotted in Fig. 8a, which indicates that 9E-BHVC always emits more intense fluorescence than DAPI at the same depth. The fluorescence intensity of 9E-BHVC and DAPI remain stable when the observation depth is less than 14 μm, but when the depth is deeper than 14 μm, both intensities show an obvious depth-related decrease. Meanwhile, the decrease of 9E-BHVC is more obvious than that of DAPI.

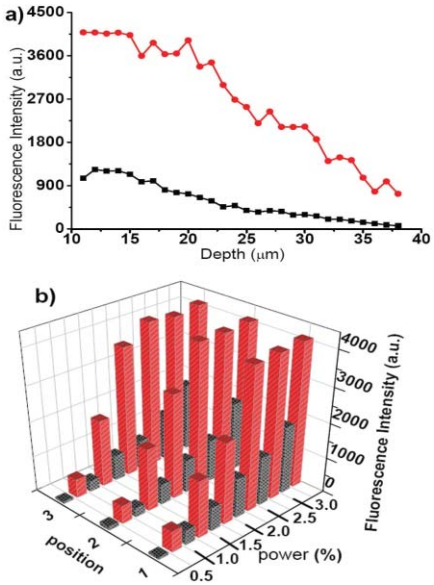

Fig. 8 Change of fluorescence intensity of 9E-BHVC and DAPI in roots with depth at 2% incident power (a) and with incident power at 18 μm (b). Data for (a) come from Video S2, those for (b) come from Video S3.† Black, DAPI. Red, 9E-BHVC. Each point shown has an error of 10%.

To investigate and compare the two-photon fluorescence intensity of 9E-BHVC and DAPI in *Arabidopsis* root, both under same incident power, the microscopic photos of the root at 18 μm stained by 9E-BHVC and DAPI under 6 levels of incident power have been obtained, and these photos were demonstrated consecutively in Video S3.† We randomly selected three nuclei indicated by arrows in Fig. 7BIIc. The intensity of 9E-BHVC and DAPI on the three nuclei under various powers was determined. The relationship between the fluorescence intensity from every nucleus of 9E-BHVC or DAPI and incident power were plotted in Fig. 8b, which indicates that 9E-BHVC always emits more intense fluorescence than DAPI at the same power.

These experimental results in double-staining *Arabidopsis* root reveal that 9E-BHVC can achieve deeper imaging or give usable fluorescence images by using a lower incident power. We consider that two factors are responsible for these results. Firstly, 9E-BHVC possesses large $\Phi \times \delta$, thus it can luminesce more intensely under the same incident power. Secondly, the fluorescent peak of 9E-BHVC is near 575 nm in the orange spectral region. Comparatively, DAPI has a lower $\Phi \times \delta$, and its 460 nm fluorescence emission in the blue-green spectral region is strongly attenuated by turbid tissue. These obvious disadvantages of conventional fluorescent probes should be a major limitation of tissue imaging when utilizing TPM; it is a primary motivation to develop superior two-photon fluorescent probes.

Conclusion

The potential of applying TPM to image living tissue has been recognized since its inception.[1a] However, according to recent reports, the low two-photon fluorescence properties of DAPI have indeed obstructed the relevant research, such as investigating meiotic events in intact living tissues. Therefore, it is necessary to find and explore a DNA fluorescent probe with not only better two-photon performance but also similar biological labeling ability to DAPI. In this article, we have presented an efficient DNA fluorescent probe, 9E-BHVC. A series of double-staining experimental results in living protoplasts, hypocotyls and roots have convincingly demonstrated that 9E-BHVC possesses tangible application potential as a new two-photon fluorescent DNA probe.

Acknowledgements

For financial support, we thank the National Science Foundation of China (50673053, 50173015, 30771091, 50990061 and 50721002) and NSFC/RGC (50218001), and Open Point of State Key Laboratory of Supramolecular Structure and Materials.

References

1 (*a*) W. Denk, J. H. Strickler and W. W. Webb, *Science*, 1990, **248**, 73–76; (*b*) B. R. Masters and P. T. C. SO, *Microsc. Res. Tech.*, 2004, **63**, 3–11.
2 S. M. Potter, *Curr. Biol.*, 1996, **6**, 1595–1598.
3 (*a*) V. E. Centonze and J. G. White, *Biophys. J.*, 1998, **75**, 2015–2024; (*b*) J. A. Feijó and N. Moreno, *Protoplasma*, 2004, **223**, 1–32.
4 M. B. Ericson, C. Simonsson, S. Guldbrand, C. Ljungblad, J. Paoli and M. J. Smedh, *J. Biophotonics*, 2008, **1**, 320–330.
5 H. C. Gerritsen and C. J. D. Grauw, *Microsc. Res. Tech.*, 1999, **47**, 206–209.
6 J. A. Feijó and G. Cox, *Micron*, 2001, **32**, 679–684.
7 (*a*) E. Martínez-Pérez, P. Shaw, S. Reader, L. Aragón-Alcaide, T. Miller and G. J. Moore, *Cell. Sci.*, 1999, **112**, 1761–1769; (*b*) A. E. Franklin, J. McElver, I. Sunjevaric, R. Rothstein, B. Bowen and W. Z. Cande, *Plant Cell*, 1999, **11**, 809–824.
8 (*a*) C. Xu and W. W. Webb, *J. Opt. Soc. Am. B*, 1996, **13**, 481–491; (*b*) C. Xu, W. Zipfel, J. B. Shear, R. Williams and W. W. Webb, *Proc. Natl. Acad. Sci. U. S. A.*, 1996, **93**, 10763–10768; (*c*) K. Kuba and S. Nakayama, *Neurosci. Res.*, 1998, **32**, 281–294; (*d*) C. D. Wilms, H. Schmidt and J. Eilers, *Cell Calcium*, 2006, **40**, 73–79.
9 (*a*) M. Göppert-Mayer, *Ann. Phys. (Leipzig)*, 1931, **9**, 273–294; (*b*) W. Kaiser and C. G. B. Garrett, *Phys. Rev. Lett.*, 1961, **7**, 229–231.
10 (*a*) Y. Q. Tian, C. Y. Chen, C. C. Yang, A. C. Young, S. H. Jang, W. C. Chen and A. K. Y. Jen, *Chem. Mater.*, 2008, **20**, 1977–1987; (*b*) H. M. Kim, B. R. Kim, J. H. Hong, J.-S. Park, K. J. Lee and B. R. Cho, *Angew. Chem., Int. Ed.*, 2007, **46**, 7445–7448; (*c*) M. Zhang, M. Yu, F. Li, M. Zhu, M. Li, Y. Gao, L. Li, Z. Liu, J. Zhang, D. Zhang, T. Yi and C. Huang, *J. Am. Chem. Soc.*, 2007, **129**, 10322–10323; (*d*) C. Barsu, R. Cheaib, S. Chambert, Y. Queneau, O. Maury, D. Cottet, H. Wege, J. Douady, Y. Bretonniere and C. Andraud, *Org. Biomol. Chem.*, 2010, **8**, 142–145; (*e*) H. Lu, L. Q. Xiong, H. Z. Liu, M. X. Yu, S. Zhen, F. Y. Li and X. Z. You, *Org. Biomol. Chem.*, 2009, **7**, 2554–2558; (*f*) Y. S. Tian, H. Y Lee, C. S. Lim, J. Park, H. M. Kim, Y. N. Shin, E. S. Kim, H. J. Jeon, S. B. Park and B. R. Cho, *Angew. Chem.*, 2009, **121**, 8171–8175; (*g*) Y. H. Gao, J. Y. Wu, Y. M. Li, P. P. Sun, H. P. Zhou, J. X. Yang, S. Y. Zhang, B. K. Jin and Y. P. Tian, *J. Am. Chem. Soc.*, 2009, **131**, 5208–5213; (*h*) P. T. C. So, C. Y. Dong, B. R. Masters and K. M. Berland, *Annu. Rev. Biomed. Eng.*, 2000, **02**, 399–429; (*i*) B. A. Reinhardt, *Chem. Mater.*, 1998, **10**, 1863–1874; (*j*) P. Yan, A. C. Millard, M. D. Wei and L. M. Leow, *J. Am. Chem. Soc.*, 2006, **128**, 11030–11031; (*k*) P. Yan, A. F. Xie, M. D. Wei and L. M. Leow, *J. Org. Chem.*, 2008, **73**, 6587–6594.
11 (*a*) L. J. Kricka, *Ann. Clin. Biochem.*, 2002, **39**, 114–129; (*b*) T. R. Gingeras, R. Higuchi, L. J. Kricka, Y. M. D. Lo and C. T. Wittwer, *lin. Chem.*, 2005, **51**, 661–671.
12 (*a*) A. Abbotto, G. Baldinib, L. Beverinaa, G. Chiricob, M. Collinib, L. D'Alfonsob, A. Diasproc, R. Magrassic, L. Nardob and G. A. Pagania, *Biophys. Chem.*, 2005, **114**, 35–41; (*b*) T. Y. Ohulchanskyy, H. E. Pudavar, S. M. Yarmoluk, V. M. Yashchuk, E. J. Bergey and P. N. Prasad, *Photochem. Photobiol.*, 2003, **77**, 138–145.
13 (*a*) C. Allain, F. Schmidt, R. Lartia, G. Bordeau, C. Fiorini-Debuisschert, F. Charra, P. Tauc and M. Teulade-Fichou, *ChemBioChem*, 2007, **8**, 424–433; (*b*) G. Bordeau, E. Faurel, C. Allain, R. Lartia, F. Schmidt, C. Fiorini-Debuisschert, F. Charra, G. Metge, P. Tauc and M.-P. Teulade-Fichou, *Nucleic Acids Symp. Ser.*, 2008, **52**, 155–156.

14 (*a*) C. C. Chang, I. C. Kuo, I. F. Ling, C. T. Chen, H. C. Chen, P. J. Lou, J. J. Lin and T. C. Chang, *Anal. Chem.*, 2004, **76**, 4490–4494; (*b*) C. C. Chang, J. F. Chu, F. J. Kao, Y. C. Chiu, P. J. Lou, H. C. Chen and T. C. Chang, *Anal. Chem.*, 2006, **78**, 2810–2815.

15 Y. L. Tsai, C. C. Chang, C. C. Kang and T. C. Chang, *J. Lumin.*, 2007, **127**, 41–47.

16 X. Liu, H. Liu, P. F. Jia, B. Zhang, J. J. Wang, N. Zhao, Y. H. Zhang and X. Q. Yu, *Chem. J. Chin. Uni.*, 2009, **30**(3), 465–467.

17 (*a*) M. K. Brennaman, T. J. Meyer and J. M. Papanikolas, *J. Phys. Chem. A*, 2004, **108**, 9938–9944; (*b*) R. B. Nair, B. M. Cullum and C. Murphy, *Inorg. Chem.*, 1997, **36**, 962–965.

18 (*a*) M. Albota, D. Beljonne and J.-L. Brédas, *Science*, 1998, **281**, 1653–1656; (*b*) W. C. Li, J. K. Feng, A. M. Ren, J. Z. Sun, X. Q. Yu and J. J. Wang, *Chem. J. Chin. Uni.*, 2010, **31**(1), 100–105.

19 M. A. Albota, C. Xu and W. W. Webb, *Appl. Opt.*, 1998, **37**(31), 7352–7356.

20 (*a*) C. C. Chang, J. F. Chu, H. H. Kuo, C. C. Kang, S. H. Lina and T. C. Chang, *J. Lumin.*, 2006, **119–120**, 84–90; (*b*) H. Y. Woo, J. W. Hong, B. Liu, A. Mikhailovsky, D. Korystov and G. C. Bazan, *J. Am. Chem. Soc.*, 2005, **127**, 820–821; (*c*) B. Strehmel, A. M. Sarker, J. H. Malpert, V. Strehmel, H. Seifert and D. C. Neckers, *J. Am. Chem. Soc.*, 1999, **121**, 1226–1236.

21 (*a*) M. C. Castex, C. Olivero, G. Pichler, D. Ade′ s, E. Cloutet and A. Siove, *Synth. Met.*, 2001, **122**, 59–61; (*b*) D. Ade′ s, V. Boucard, E. Cloutet, A. Siove, C. Olivero, M. C. Castex and G. Pichler, *J. Appl. Phys.*, 2000, **87**, 7290–7293.

22 (*a*) K. Rotkiewicz, K. H. Grellman and Z. R. Grabowski, *Chem. Phys. Lett.*, 1973, **19**, 315–318; (*b*) W. Rettig, *Angew. Chem., Int. Ed. Engl.*, 1986, **25**, 971–988; (*c*) A. Nag and K. Bhattacharyya, *Chem. Phys. Lett.*, 1990, **169**, 12–16; (*d*) G. R. Fleming, G. Portor, R. J. Robbins and J. A. Synowiec, *Chem. Phys. Lett.*, 1977, **52**, 228–232; (*e*) G. W. Robinson, R. J. Robbins, G. R. Fleming, J. M. Morris, A. E. W. Knight and R. J. S. Morrison, *J. Am. Chem. Soc.*, 1978, **100**, 7145–7150.

23 (*a*) M. Chauhan and F. Arjmand, *Chem. Biodiversity*, 2006, **3**, 660–676; (*b*) Z. D. Xu, H. Liu, M. Wang, S. L. Xiao, M. Yang and X. H. Bu, *J. Inorg. Biochem.*, 2002, **90**, 79–84.

24 (*a*) M. Mariappan and B. G. Maiya, *Eur. J. Inorg. Chem.*, 2005, 2164–2173; (*b*) R. Bera, B. K. Sahoo, K. S. Ghosh and S. Dasgupta, *Int. J. Biol. Macromol.*, 2008, **42**, 14–21; (*c*) D. L. Ma and C. M. Che, *Chem.–Eur. J.*, 2003, **9**, 6133–6144.

25 (*a*) M. Hranjec, K. Starcevic, I. Piantanida, M. Kralj, M. Marjanovic, M. Hasani, G. Westman and G. Karminski-Zamola, *Eur. J. Med. Chem.*, 2008, **43**, 2877–2890; (*b*) X. Jiang, L. Shang, Z. X. Wang and S. Dong, *Biophys. Chem.*, 2005, **118**, 42–50.

26 (*a*) S. S. Palayangoda, X. Cai, R. M. Adhikari and D. C. Neckers, *Org. Lett.*, 2008, **10**, 281–284; (*b*) C. Reichardt, *Chem. Rev.*, 1994, **94**, 2319–2358; (*c*) D. W. Allen and X. Li, *J. Chem. Soc., Perkin Trans. 2*, 1997, 1099–1104; (*d*) T. Soujanya, R. W. Fessenden and A. Samanta, *J. Phys. Chem.*, 1996, **100**, 3507–3512.

27 (*a*) Y. Guan, R. Shi, X. M. Li, M. P. Zhao and Y. Z. Li, *J. Phys. Chem. B*, 2007, **111**, 7336–7344; (*b*) B. D. Wang, Z. Y. Yang and T. R. Li, *Bioorg. Med. Chem.*, 2006, **14**, 6012–6021.

28 (*a*) F. A. Tanious, J. M. Veal, H. Buczak, L. S. Ratmeyer and W. D. Wilson, *Biochemistry*, 1992, **31**, 3103–3112; (*b*) W. D. Wilson, F. A. Tanious, H. J. Barton, R. L. Jones, K. Fox, R. L. Wydra and L. Strekowsk, *Biochemistry*, 1990, **29**, 8452–8461.

29 (*a*) J. Liu, H. Zhang, C. H. Chen, H. Deng, T. B. Lu and L. N. Ji, *Dalton Trans.*, 2003, 114–119; (*b*) C. L. Liu, J. Y. Zhou, Q. X. Li, L. J. Wang, Z. R. Liao and H. B. Xu, *J. Inorg. Biochem.*, 1999, **75**, 233–240.

30 E. López, M. Pradillo, C. Romero, J. L. Santos and N. Cuñado, *Chromosome Res.*, 2008, **16**, 701–708.

